J. Fluid Mech. (1976), *vol.* 77, *part* 3, *pp.* 473–497
Printed in Great Britain

Measurements with a pulsed-wire and a hot-wire anemometer in the highly turbulent wake of a normal flat plate

By L. J. S. BRADBURY
Mechanical Engineering Department, University of Surrey, Guildford, England

(Received 25 November 1975)

This paper describes an investigation into the response of both the pulsed-wire anemometer and the hot-wire anemometer in a highly turbulent flow. The first part of the paper is concerned with a theoretical study of some aspects of the response of these instruments in a highly turbulent flow. It is shown that, under normal operating conditions, the pulsed-wire anemometer should give mean velocity and longitudinal turbulent intensity estimates to an accuracy of better than 10 % without any restriction on turbulence level. However, to attain this accuracy in measurements of turbulent intensities normal to the mean flow direction, there is a lower limit on the turbulent intensity of about 50 %. An analysis is then carried out of the behaviour of the hot-wire anemometer in a highly turbulent flow. It is found that the large errors that are known to develop are very sensitive to the precise structure of the turbulence, so that even qualitative use of hot-wire data in such flows is not feasible. Some brief comments on the possibility of improving the accuracy of the hot-wire anemometer are then given.

The second half of the paper describes some comparative measurements in the highly turbulent flow immediately downstream of a normal flat plate. It is shown that, although it is not possible to interpret the hot-wire results on their own, it is possible to calculate the hot-wire response with a surprising degree of accuracy using the results from the pulsed-wire anemometer. This provides a rather indirect but none the less welcome check on the accuracy of the pulsed-wire results, which, in this very highly turbulent flow, have a certain interest in their own right.

1. Introduction

For many practical reasons, there has been a considerable increase in interest in highly turbulent flows in recent years. However, experimental investigations of these flows have been hampered by the absence of suitable velocity measuring devices and the pulsed-wire anemometer was developed in an attempt to fill this gap in instrumentation. The principles of this instrument and its early development have already been described (Bradbury & Castro 1971) but, since then, it has been the subject of considerable development. Some of these developments have already been discussed along with some examples of the instrument's use

in a study of the flow past a normal flat plate (Bradbury & Moss 1975). This investigation of the highly turbulent wake flow behind a bluff body is continuing but, at its outset, it seemed to offer an opportunity of a separate study into the behaviour of not only the pulsed-wire anemometer but also the hot-wire anemometer in a highly turbulent flow. The present paper describes the results of this peripheral investigation.

As is the case with any technique, there are many factors which influence the accuracy of the pulsed-wire anemometer and it is only by the systematic study of these factors that proper confidence in the technique can be established. One of the most important of these factors is departures from the ideal yaw response of the instrument. The effect of these departures is considered in § 2 for the case when the mean velocity is normal to the plane of the probe and also for the case when the mean velocity is in the plane of the probe. Appendix B contains a discussion of the effect of yaw-response imperfections on measured probability density distributions.

Section 3 considers the behaviour of the hot-wire anemometer in a highly turbulent flow. The hot-wire anemometer has been the most successful instrument so far developed for studying turbulent flows but a serious limitation is that it is properly applicable only to flows with low turbulence levels. Nevertheless, because of the previous absence of any alternative, it has been used on many occasions in flows with very high turbulence levels. The investigators concerned have invariably been well aware that the instrument is subject to serious errors in such circumstances and have therefore tended to interpret the results only in a very qualitative way (see, for example, Tani, Iuchi & Komoda 1961; Gaster 1971). However, § 3 contains a theoretical investigation of the response of a linearized hot-wire anemometer to a non-isotropic turbulent flow under the assumption that the probability density distribution of the velocity fluctuation can be approximated by uncorrelated Gaussian distributions. The purpose of this study was twofold. In the first place, there seemed the remote possibility of developing a scheme of simple corrections for hot-wire anemometer readings so that its use in highly turbulent flows might be somewhat extended. This exercise was not undertaken with any great expectation of success and, indeed, this pessimistic view was fully confirmed by the results of the analysis, which show how sensitive hot-wire anemometer results are to the precise structure of the turbulence in a highly turbulent flow. However, the second aim of the analysis, accepting failure of the first, was to provide an approximate method of calculating the hot-wire anemometer response using the pulsed-wire anemometer data. By this rather tortuous process, it was hoped to provide some independent assessment of the accuracy of the pulsed-wire results. An obvious alternative to this procedure would have been to use a laser anemometer. Such comparative measurements with a laser anemometer are planned for the future using the photon correlation technique but, apart from the non-availability of such equipment at the time of the present measurements, it is worth noting that there are ambiguities in analysing laser-Doppler anemometer results in highly turbulent flow because of the coupling between the turbulent flow field and the convection of particles into the scattering volume. The rate of arrival of particles in a scattering

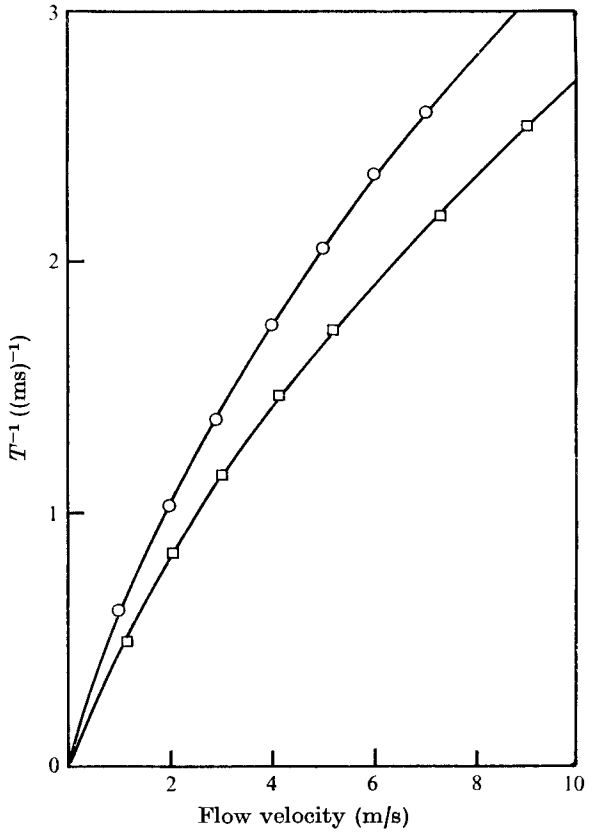

FIGURE 1. Typical pulsed-wire anemometer calibration. —, least-squares fit of (1).

volume is proportional to the magnitude of the velocity vector and the frontal area of the effective scattering volume resolved normal to this vector and the problem of this bias needs careful consideration if accurate results are to be obtained.

Section 4 contains the results of the comparative measurements. The measurements were made in the wake region immediately downstream of the nominally two-dimensional flow past a normal flat plate. The results of the measurements confirm how drastically the hot wire can be affected by high turbulence levels, so that even the most general interpretation of hot-wire data in such flows cannot usefully be undertaken. However, it is shown that, using the results of the pulsed-wire anemometer measurements, the hot-wire anemometer response can be calculated using the analysis contained in §3: the agreement with experimental results is very good. This is a process that would normally be quite useless but, in the present circumstances, it does give some indirect confirmation of the general accuracy of the pulsed-wire anemometer results. These results have a certain interest in their own right although much remains to be done in studying the near-wake region behind the flat plate. A final point to emerge from the experiments is that in regions of low turbulence good agreement was obtained between

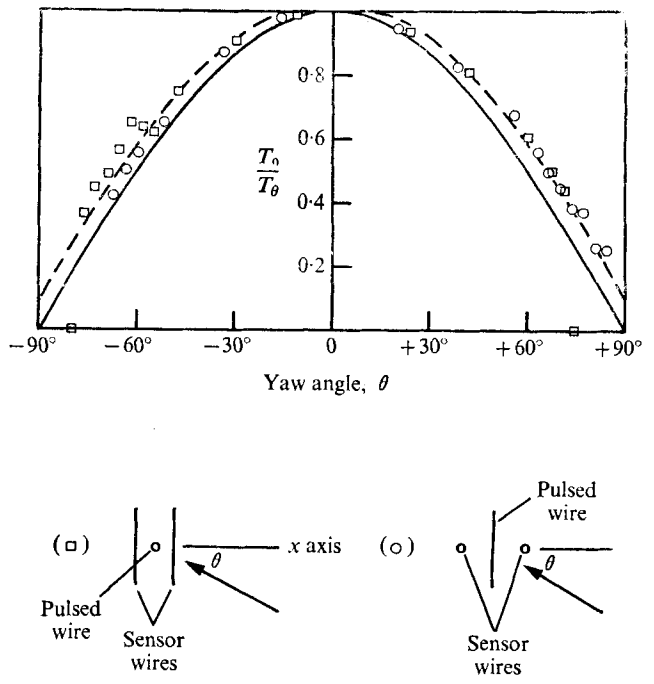

FIGURE 2. Typical pulsed-wire anemometer yaw response. —, $\cos\theta$; – – –, $\cos\theta\,(1+\epsilon\tan\theta)$ with $\epsilon = 0{\cdot}1$.

the pulsed-wire and hot-wire anemometers, which provides yet further guidance as to the overall consistency and accuracy of the experimental data.

2. The pulsed-wire anemometer in highly turbulent flow

The present pulsed-wire anemometer uses probes that are of similar geometry to those used by Bradbury & Castro (1971). The times of flight are obtained from the use of differentiated sensor-wire signals as described in the earlier work but the circuitry for manipulating the signals is now highly developed and an entirely self-contained instrument has been constructed which can be operated on-line with a variety of mini-computers and programmable desk calculators.

Although the responses of the probes used in the present experiments are superficially similar to those obtained previously, the consistency of calibrations is of a higher magnitude altogether and it is therefore important to re-examine these to assess the likely magnitude of the measurement errors.

Figure 1 shows a typical calibration of the two sensor wires on a probe. The calibrations for the two sensor wires are not the same because of differences in the spacings between the pulsed wire and the two sensor wires. A good empirical fit to the calibrations is found to be

$$U = A/T + B/T^2, \tag{1}$$

where U is the air velocity and T is the time of flight. A and B are constants that can be determined by a least-squares fit to the data and the solid lines shown in

figure 1 are curves obtained in this way. The appearance in the calibrations of some nonlinearity between the velocity and the reciprocal of the time of flight is due primarily to the effects of thermal diffusion but, because of the contribution of other effects, it is not possible to predict the form of this nonlinearity in any simple way, so that the simple expedient of adopting an empirical fit has been followed. The nonlinearity is of no great practical significance because each individual reading is easily linearized in on-line operation. However, more important characteristics as far as the inherent accuracy of the technique is concerned are departures from the ideal yaw response of the instrument. Figure 2 shows a yaw response obtained with the present system which illustrates a number of important features. The results in figure 2 were obtained by yawing the probe about two axes at right angles to one another as defined in figure 2. First, the yaw response does not extend to $\pm 90°$ owing to the finite length of the wires but, typically, a response is maintained up to yaw angles of about $\pm 70°$. This limit on the extent of the yaw response due to the length of the wires will be subsequently referred to as the finite yaw response. It should also be noted that the yaw response does not follow the ideal cosine-law response but lies somewhat above it. This is again primarily due to the effects of diffusion. For the purpose of estimating the errors due to departures from the ideal yaw response, it seems that the yaw response can be reasonably represented by the expression

$$T_0/T_\theta = \cos\theta + \epsilon \sin\theta, \tag{2}$$

where T_0 and T_θ are the mean times of flight at zero yaw angle and at a yaw angle θ respectively. From the experimental data, ϵ seems to be about 0·1. There is obviously no physical basis behind this expression; it simply seems to fit the data in the range of velocities from about 0·25 m/s to 15 m/s over which the pulsed-wire anemometer can be used. The final point to note about the yaw response is that, for the results represented by the square symbols, there is some irregularity in the variation of the mean time of flight with yaw angles in the neighbourhood of $-60°$. This is accompanied by an increase in the fluctuations in the time of flight amounting to a standard deviation of about 15 % of the mean time of flight. This arises from the flow around the wire supports. These are asymmetric, so that the results for positive yaw angles do not exhibit this irregularity nor do the results represented by the circular symbols. It would be possible to reduce this effect by improving the layout of the probe geometry. It is also worth noting that, owing to electronic noise, the standard deviation of the flight times in laminar flow is normally between 1 and 2 % of the mean value and this sets the lower limit to turbulent intensities that can be measured with the instrument.

The above features of the yaw response are the most important sources of error in using a pulsed-wire anemometer and we need to obtain estimates of the likely magnitude of these errors. If we neglect the probe interference effect, the mean velocity component in the x direction (normal to the plane of the probe) recorded by the pulsed-wire anemometer (figure 2) is given by

$$\overline{U}_a = \iiint_{\text{cones}} u\left(1+\epsilon\frac{v_r}{u}\right) p(u,v,w)\,du\,dv\,dw \tag{3}$$

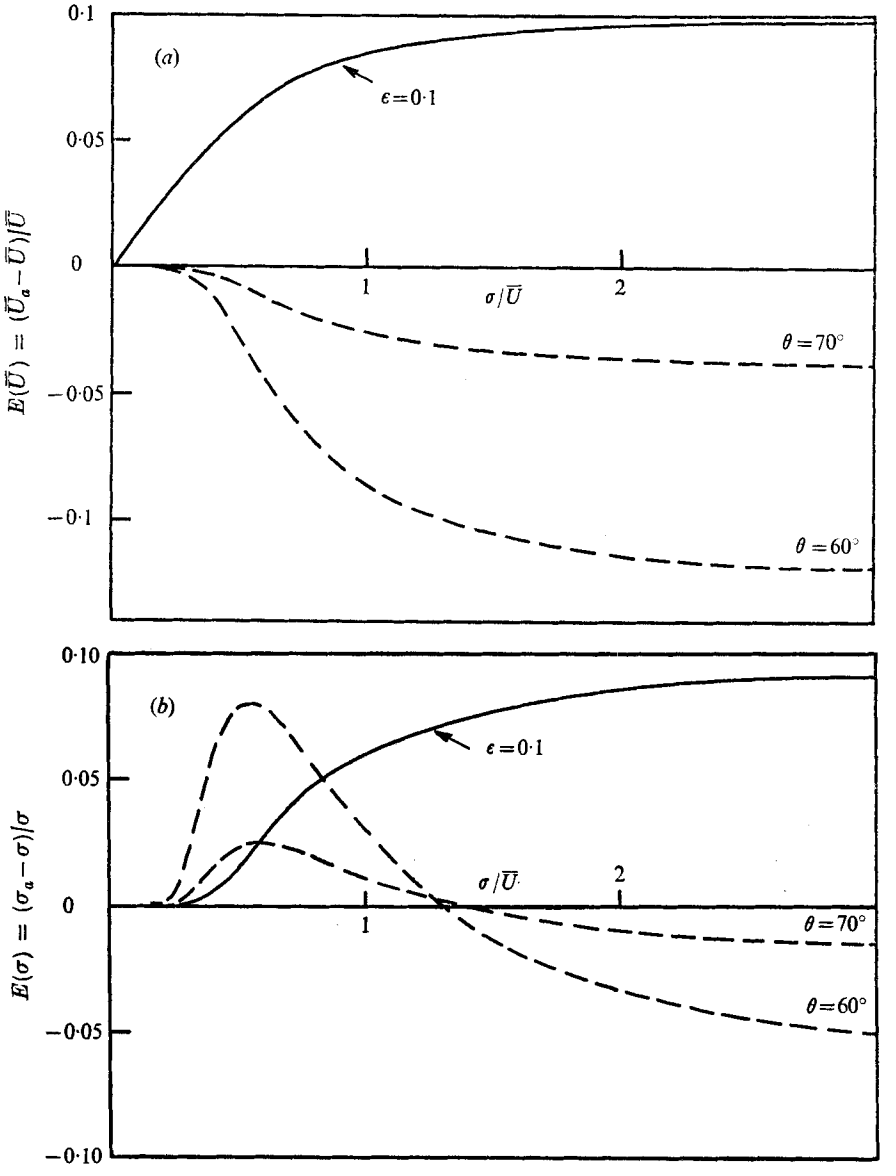

FIGURE 3. Errors in estimates of (*a*) mean velocity and (*b*) longitudinal turbulent intensity from a pulsed-wire anemometer. —, error due to departure from cosine law; – – –, error due to finite yaw response.

and the mean square of the velocity is

$$\overline{U}_a^2 = \iiint_{\text{cones}} u^2 \left(1+\epsilon\frac{v_r}{|u|}\right)^2 p(u,v,w)\,du\,dv\,dw, \tag{4}$$

where $p(u,v,w)$ is the joint probability density distribution of the velocity components u, v and w in the x, y and z directions respectively. v_r is equal to $(v^2+w^2)^{\frac{1}{2}}$ and the limits of integration are such as to restrict the velocities to lie

within the cone angles of the finite yaw response. Equations (3) and (4) correspond to the values obtained by treating heat tracers which miss the sensor wires altogether as zero-velocity samples.

For the purposes of estimating the errors, the joint probability density distribution will be taken to be represented by an isotropic uncorrelated Gaussian model so that

$$p(u,v,w) = \frac{1}{(2\pi\sigma^2)^{\frac{3}{2}}} \exp\left(\frac{-(u-\overline{U})^2-(v-\overline{V})^2-w^2}{2\sigma^2}\right), \tag{5}$$

where $\overline{U}$ and $\overline{V}$ are the mean velocities in the x and y directions respectively and σ is the r.m.s. turbulent intensity. Two cases will be considered: first, when the mean velocity is in the x direction; second, when it is in the y direction. In both cases, the influence of the finite yaw response and departures from the cosine law will be considered separately. This greatly simplifies the analysis and also emphasizes the relative contributions of the two effects.

The errors due to the finite yaw response only (i.e. $\epsilon = 0$) in the case when $\overline{V} = 0$ have already been discussed by Bradbury & Castro (1971). Analytic expressions for the errors were obtained and, for completeness, the results of this analysis are shown in figures 3 (*a*) and (*b*) for errors in mean velocity and turbulent intensity respectively for two values of the finite yaw response, namely 60° and 70°. In these figures, the suffix a refers to the apparent values recorded by the pulsed-wire anemometer and the quantities without suffixes are the true values. If we assume that the yaw response as given in (2) now extends to 90°, it is again possible to obtain analytic expressions for the errors due to departures from the cosine law. In the case of the mean velocity, we obtain

$$E(\overline{U}) = \frac{\overline{U}_a - \overline{U}}{\overline{U}} = \epsilon\left(\frac{\pi}{2}\right)^{\frac{1}{2}} \frac{\sigma}{\overline{U}} \operatorname{erf}\left(\frac{\frac{1}{2}\overline{U}}{(2\sigma^2)^{\frac{1}{2}}}\right) \tag{6}$$

and the error in the turbulent intensity becomes

$$E(\sigma) = \frac{\sigma_a - \sigma}{\sigma} = \left\{1 + 2\epsilon \exp\left(\frac{-\overline{U}^2}{2\sigma^2}\right) + \epsilon^2\left[2 - \frac{\pi}{2}\left(\operatorname{erf}\frac{\overline{U}}{(2\sigma^2)^{\frac{1}{2}}}\right)^2\right]\right\}^{\frac{1}{2}} - 1. \tag{7}$$

These expressions are plotted in figures 3 (*a*) and (*b*) respectively with $\epsilon = 0{\cdot}1$. In the case of the estimates of mean velocity, the errors due to the finite yaw response are of opposite sign to those due to departures from the cosine law. With probes having a yaw response of between 60° and 70°, it would seem therefore that the errors in mean velocity due to the combined effects at high turbulence levels should not be more than about 5 %. The errors in the estimates of turbulent intensity are of a more complicated form but, in this case, it would appear that an accuracy of better than 10 % is quite feasible.

The case in which the mean velocity is in the plane of the probe will now be considered. This situation arises in measurements of the transverse components of the turbulent intensities. Under these circumstances, the probe gives a correct zero mean velocity estimate and it is only necessary to consider the errors in intensity measurements. The effect of finite yaw angles only is considered in appendix A, where it is shown that (4) with (5) can only be evaluated numerically. The results of this numerical integration are shown in figure 4 for the cases of yaw

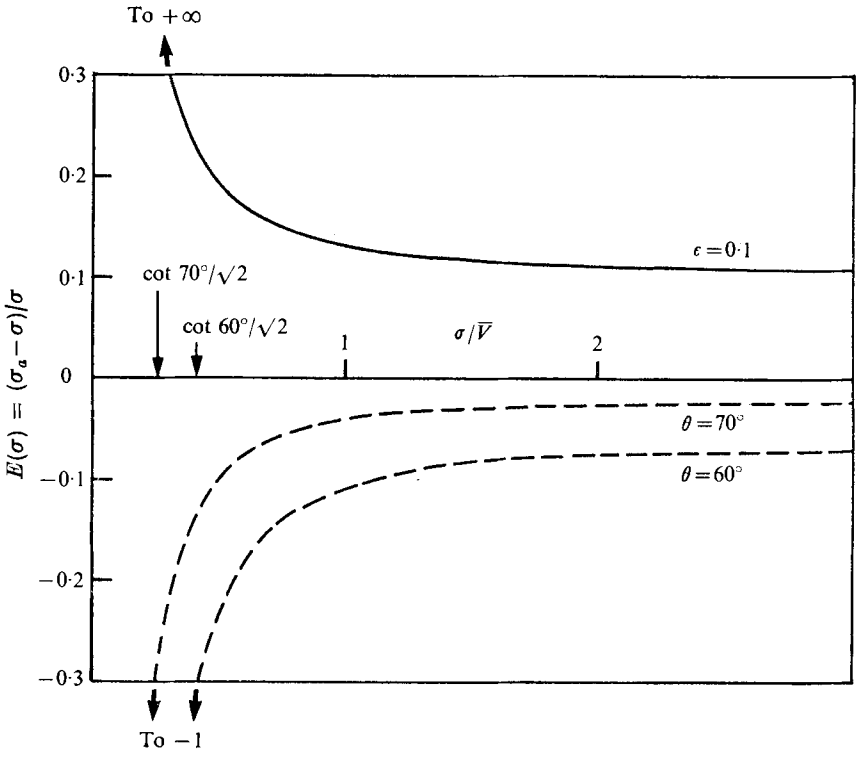

FIGURE 4. Errors in estimates of transverse turbulent intensity from a pulsed-wire anemometer. Curves as in figure 3.

angle limits of 60° and 70°. Clearly, when the intensity is very low, the probe picks up very few of the tracers of heated air and the error is large. However, as the intensity increases, the accuracy improves, and finally σ_a^2/σ^2 approaches $1 - \cos^2\theta$ as the mean velocity tends to zero. The maximum in the curve of $u^2p(u)$ for a Gaussian process occurs when $u/\sigma = \sqrt{2}$, so that we might expect σ_a^2/σ^2 to be approximately 0·5 (or $E(\sigma) = 1/\sqrt{2} - 1$) when σ/V is equal to $\cot\theta/\sqrt{2}$ and reference to figure 4 shows that this is roughly the case.

The effect of the departures from the cosine law is now considered for the case of a yaw response that extends up to 90°. In this case, after a good deal of manipulation, (4) gives

$$E(\sigma) = \frac{\sigma_a - \sigma}{\sigma} = \left[1 + \epsilon f\left(\frac{\sigma}{\overline{V}}\right) + \epsilon^2\left(2 + \frac{\overline{V}^2}{\sigma^2}\right)\right]^{\frac{1}{2}} - 1, \tag{8}$$

where $$f\left(\frac{\sigma}{\overline{V}}\right) = \frac{8\exp(-\overline{V}^2/2\sigma^2)}{\pi}\int_0^{\frac{1}{2}\pi} \exp\left(\frac{\overline{V}^2\sin^2\theta}{2\sigma^2}\right)\left(\frac{1}{2} + \frac{\overline{V}^2\sin^2\theta}{2\sigma^2}\right) d\theta.$$

For general values of $\sigma/\overline{V}$, this integral has also to be evaluated numerically. The errors in intensity estimates from (8) are plotted in figure 4. The errors due to the finite yaw limit and to departures from the cosine law are again of opposite sign and since (8) will overestimate the errors from cosine-law departures, particularly at the lower values of $\sigma/\overline{V}$, it would seem that transverse intensity measurements can be made to an accuracy of better than about 10 % once the turbulence level

rises above about 50 %. For lower intensities than this, it is possible in principle to obtain these transverse components, and also shear stresses, by taking measurements at, say, $\pm 45°$ to the mean velocity direction in addition to the ordinary measurement of intensity in the direction of the mean velocity. However, further analysis is necessary to establish the sensitivity of these measurements to the yaw response characteristics.

The purpose of the preceding discussion has been to establish the magnitude of errors in estimates of mean velocity and turbulent intensity that might arise with the pulsed-wire anemometer. In estimating these errors using (3) and (4), it is interesting to note that it is unnecessary to calculate the form of the probability density distributions recorded by the pulsed-wire anemometer. However, there are occasions when these probability density distributions might be of interest, and appendix B contains a discussion of the effects on these distributions of the finite yaw limit and departures from the cosine law.

3. The hot-wire anemometer in highly turbulent flow

In the experiments to be described in § 4, the output from the hot-wire anemometer was linearized, so that the assumption of a linearized wire output will be used in the following analysis. For simplicity, it will also be assumed that only the component of velocity normal to the axis of the wire is effective in cooling the wire. In these circumstances, the apparent mean velocity recorded by a hot-wire anemometer is

$$\overline{U}_a = \int_{-\infty}^{\infty}\int_{-\infty}^{\infty}\int_{-\infty}^{\infty} (u^2+v^2)^{\frac{1}{2}}\, p(u,v,w)\,du\,dv\,dw, \tag{9}$$

where w is the component of velocity along the axis of the wire. This expression allows for the fact that the hot wire responds only to the modulus of the velocity vector in the plane normal to its axis and is not capable of resolving changes in the flow direction in this plane. As in § 2, we shall now assume a turbulence model in which the probability density distributions of the three velocity components are uncorrelated with one another and can be represented by Gaussian distributions. The w component of velocity then plays no further role in the analysis. The mean velocity is taken to be in the direction of the u component and the r.m.s. intensity of the u-component fluctuations is taken to be σ. The turbulence is not assumed to be isotropic and the v-component intensity is assumed to be $k\sigma$, where k can be either greater than or less than unity. In these circumstances (9) becomes

$$\overline{U}_a = \frac{1}{2\pi k\sigma^2}\int_{-\infty}^{\infty}\int_{-\infty}^{\infty} (u^2+v^2)^{\frac{1}{2}} \exp\left(\frac{-(u-\overline{U})^2}{2\sigma^2}\right)\exp\left(\frac{-v^2}{2k^2\sigma^2}\right)du\,dv, \tag{10}$$

where $\overline{U}$ is the true mean velocity. If we introduce a radial velocity $v_r = (u^2+v^2)^{\frac{1}{2}}$ so that $u = v_r\cos\theta$ and $v = v_r\sin\theta$ then (10) can be reduced to

$$\frac{\overline{U}_a}{\overline{U}} = \left(\frac{2}{\pi}\right)^{\frac{1}{2}} \frac{\exp(-\overline{U}^2/2\sigma^2)}{k}\int_0^{\frac{1}{2}\pi}\left\{\frac{\overline{U}}{\sigma}\frac{\cos^2\theta}{[1+\sin^2\theta(k^{-2}-1)]}+\frac{\sigma}{\overline{U}}\right\} \times \frac{\exp(\overline{U}^2\cos^2\theta/\{2\sigma^2[1+\sin^2\theta(k^{-2}-1)]\})}{[1+\sin^2\theta(k^{-2}-1)]^{\frac{3}{2}}}\,d\theta. \tag{11}$$

It does not seem possible to integrate this directly although it is possible to obtain analytic asymptotic expansions for both $\overline{U}/\sigma \to 0$ and $\overline{U}/\sigma \to \infty$ when $k = 1$, $k = 0$ and $k = \infty$. However, there is nothing of intrinsic interest in these expressions so the discussion below is based on the straightfoward numerical evaluation of this integral. It is perhaps worth noting that when $\overline{U} = 0$ equation (11) becomes

$$\frac{\overline{U}_a}{\sigma} = \frac{1}{k}\left(\frac{2}{\pi}\right)^{\frac{1}{2}} \int_0^{\frac{1}{2}\pi} \frac{d\theta}{[1+\sin^2\theta(k^{-2}-1)]^{\frac{1}{2}}}.$$

In other words, as one would expect, the hot-wire anemometer records a finite value of the mean velocity when $\overline{U} = 0$. In particular, we have (*a*) $\overline{U}_a/\sigma = (\frac{1}{2}\pi)^{\frac{1}{2}}$ when $k = 1$, (*b*) $\overline{U}_a/\sigma = (2/\pi)^{\frac{1}{2}}$ when $k = 0$ and (*c*) $\overline{U}_a/\sigma \sim k(2/\pi)^{\frac{1}{2}}$ when $k \to \infty$.

Equation (11) enables the effect of turbulence on the mean velocity estimates to be computed. In order to study the effect on the measured values of the turbulent intensities themselves, we require the mean-square output from the hot wire. This is simply given by

$$(\overline{U}^2)_a = \overline{U}^2 + (1+k^2)\sigma^2 \tag{12}$$

and the apparent u-component turbulent intensity is then

$$\sigma_a = [(\overline{U}^2)_a - (\overline{U}_a)^2]^{\frac{1}{2}}. \tag{13}$$

One of the intentions of the present investigations was to examine the possibility of developing corrections for hot-wire results which might extend the usefulness of the instrument in flows with high levels of turbulence. Thus the results obtained from evaluating the integral in (11) have been combined with (12) and (13) to produce figures 5(*a*) and (*b*). These show the ratios of the true to the measured values of the mean velocity and turbulent intensity respectively as a function of the ratio of the measured turbulent intensity to the measured mean velocity. The calculations have been carried out for values of $k = 0{\cdot}5$, 1 and 2, which covers most practical examples of turbulent flows. It should be noted that when $\overline{U} = 0$ with $k = 1$, $\sigma_a/U_a = (4/\pi - 1)^{\frac{1}{2}}$ and $\sigma/\sigma_a = 1/(2-\frac{1}{2}\pi)^{\frac{1}{2}}$.

Figure 5(*a*) shows the variation of the correction factor for mean velocity as a function of the measured ratio of the turbulent intensity to the mean velocity. For errors of less than 10 %, it seems that the turbulent intensity ratio should not exceed between 20 and 30 %. However, above this ratio, the variation of the correction factor with the intensity ratio is very rapid and very sensitive to the value of k. It is thus quite clear that there is no chance of sensibly attempting to correct hot-wire results, particularly when the corrections will have an added sensitivity to variations in the form of the probability density distributions. This conclusion corresponds closely to that reached by Tutu & Chevray (1975) in a more detailed analysis of the behaviour of an X-probe.

As far as the results for the intensity correction factor in figure 5(*b*) are concerned, most of the above comments on mean velocity corrections apply again. However, whereas the hot-wire anemometer always records a mean velocity that is larger than the true mean velocity, the error in the apparent turbulent intensity can take either sign depending on the magnitude of the transverse (v) component of the turbulent intensity relative to the longitudinal intensity. The ends of the

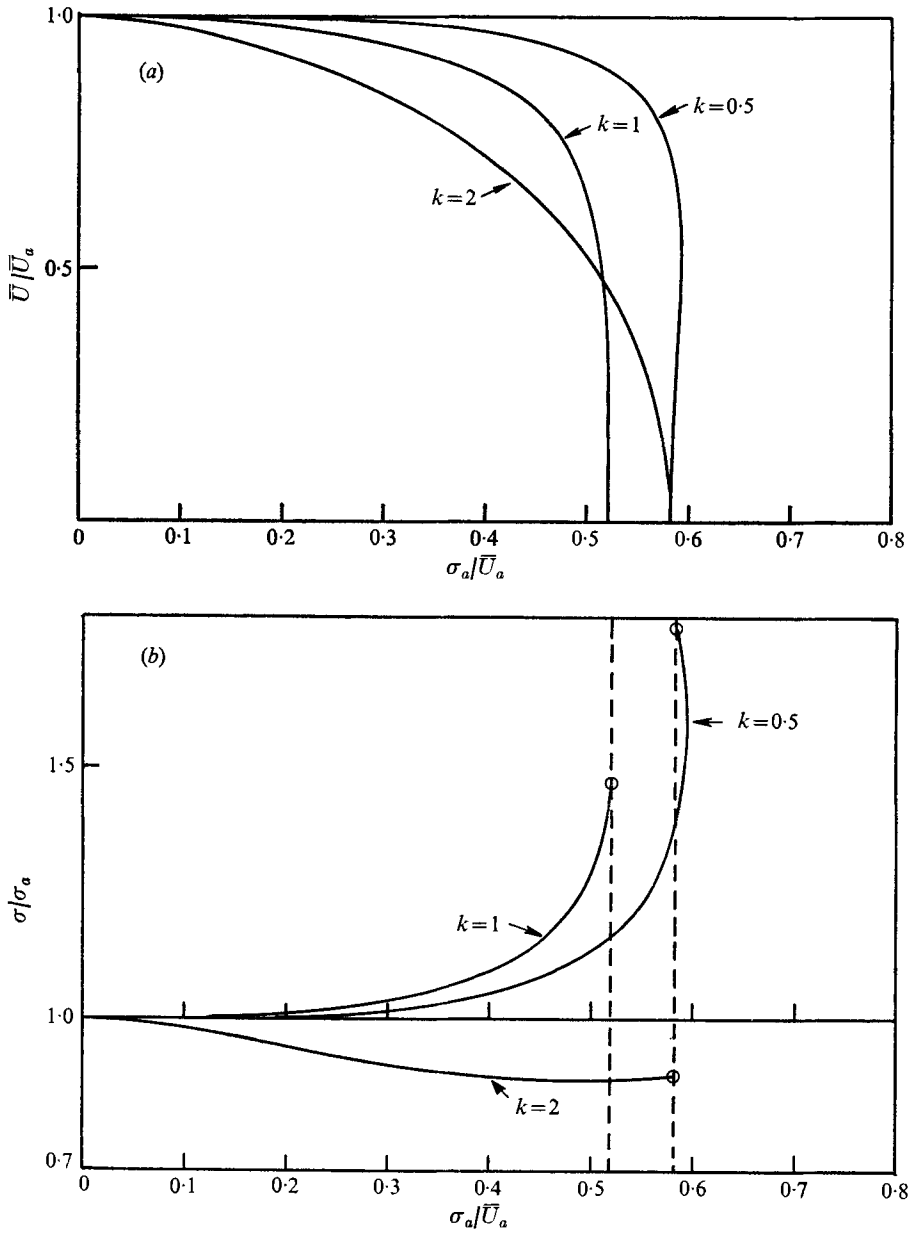

FIGURE 5. Errors in estimates of (*a*) mean velocity and (*b*) turbulent intensity from a hot-wire anemometer.

curves in figure 5 (*b*) marked with the circular symbols correspond to the correction factors when the true mean velocity is zero. It is also interesting to note that multivalued correction factors arise.

The preceding analysis confirms the long accepted view that the results of hot-wire measurements in turbulent flows with intensities greater than about 20–30 % must be treated with caution. However, there are a number of techniques

which may be used to improve the applicability of hot wires to highly turbulent flows. One of these is to use an array of hot wires from which it is possible, in principle, to follow the instantaneous velocity vector. However, there are considerable practical difficulties with this approach arising from the stability of the calibrations and the effect of such factors as probe interference. To the author's knowledge, there has never been a convincing demonstration that this technique is workable. An alternative is to use the type of probe described by Guenkel, Patel & Weber (1971) and again more recently by Cook & Redfearn (1976). This probe uses two parallel hot wires mounted in a small shroud. It is capable of sensing flow direction and it is also apparently possible to produce a reasonably unambiguous yaw response. This is a promising technique but the work so far has only really established the feasibility of the technique and a good deal remains to be done before its potential and limitations can be assessed properly. There is also the possibility of using a technique similar to that described briefly by Downing (1972). If a fine wire is mounted close and at right angles to the hot wire, it may be used as a resistance thermometer to sense the presence or otherwise of the wake of the hot wire and thus to rectify the hot-wire signal when a flow reversal occurs. The probe clearly is similar to a pulsed-wire probe although only one sensor wire is required. Although this technique would remove the ambiguity from flow reversal, it does nothing to reduce the basic nonlinearity arising from the hot wire's response to the modulus of the velocity vector. However, since there is little doubt that such a technique could be developed into a practical form without undue difficulty, it is perhaps interesting to examine the errors that would arise with a hot wire used in this way. In this case, (9) becomes

$$\overline{U}_a = \int_{-\infty}^{\infty}\int_{-\infty}^{\infty}\int_{-\infty}^{\infty} (\operatorname{sgn} u)\,(u^2+v^2)^{\frac{1}{2}}\,p(u,v,w)\,du\,dv\,dw.$$

Again, for the case of an uncorrelated Gaussian turbulence model, we obtain

$$\begin{aligned}\frac{\overline{U}_a}{\overline{U}} = \frac{2\exp(-\overline{U}^2/2\sigma^2)}{\pi k}\int_0^{\frac{1}{2}\pi}\Bigg\{&\frac{\cos\theta}{[1+\sin^2\theta(k^{-2}-1)]^2}\\ &+\left(\frac{\pi}{2}\right)^{\frac{1}{2}}\operatorname{erf}\frac{\overline{U}\cos\theta}{(2\sigma^2)^{\frac{1}{2}}[1+\sin^2\theta(k^{-2}-1)]^{\frac{1}{2}}}\\ &\times\left(\frac{(\overline{U}/\sigma)\cos^2\theta}{1+\sin^2\theta(k^{-2}-1)}+\frac{\sigma}{\overline{U}}\right)\frac{\exp(\overline{U}^2\cos^2\theta/2\sigma^2(1+\sin^2\theta(k^{-2}-1)))}{(1+\sin^2\theta(k^{-2}-1))^{\frac{3}{2}}}\Bigg\}d\theta. \quad (14)\end{aligned}$$

The expression for the mean-square velocity remains the same as before, i.e. equation (12). Although (14) is again not generally integrable, the limiting case as $\sigma/\overline{U}\to\infty$ is

$$\begin{aligned}\frac{\overline{U}_a}{\overline{U}} &\to \frac{4}{\pi k}\int_0^{\frac{1}{2}\pi}\frac{\cos\theta}{(1+\sin^2\theta(k^{-2}-1))^2}\,d\theta\\ &= \begin{cases}\dfrac{2}{\pi}\left[\dfrac{1}{k(k^{-2}-1)^{\frac{1}{2}}}\tan^{-1}(k^{-2}-1)^{\frac{1}{2}}+k\right] & \text{for} \quad k<1,\\ \dfrac{2}{\pi}\left[\dfrac{1}{k(1-k^{-2})^{\frac{1}{2}}}\tanh^{-1}(1-k^{-2})^{\frac{1}{2}}+k\right] & \text{for} \quad k>1,\end{cases}\end{aligned}$$

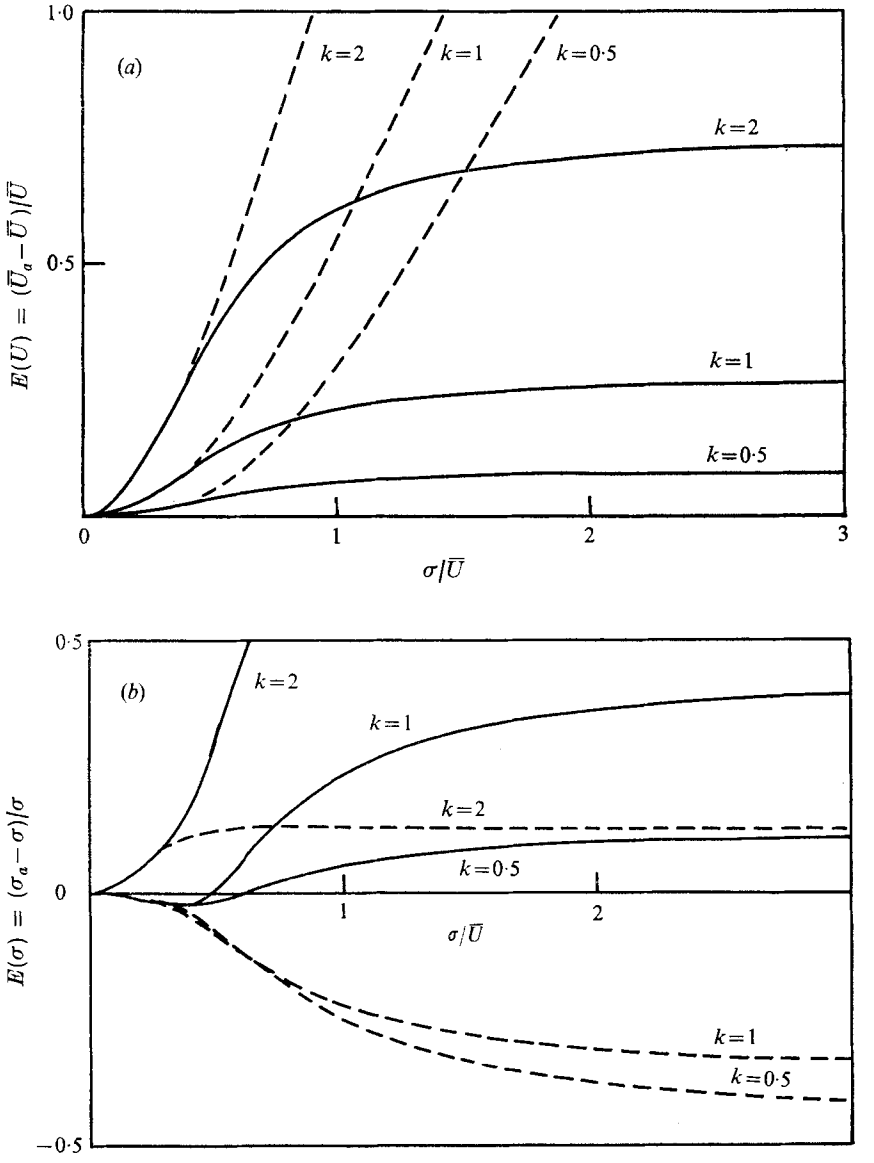

FIGURE 6. Errors in estimates of (*a*) mean velocity and (*b*) turbulent intensity from a 'rectified' hot-wire anemometer. —, 'rectified' wire; – – –, unrectified wire.

and, for the apparent intensity,

$$\sigma_a/\sigma \to (1+k^2)^{\frac{1}{2}}.$$

Equation (14) has been evaluated numerically and, in conjunction with (12), it has been used to construct figures 6(*a*) and (*b*), which show the errors in the estimates of the mean velocity and turbulent intensity that would be obtained from a 'rectified' hot-wire anemometer as a function of the ratio of the true intensity to the true mean velocity. The results have again been computed for

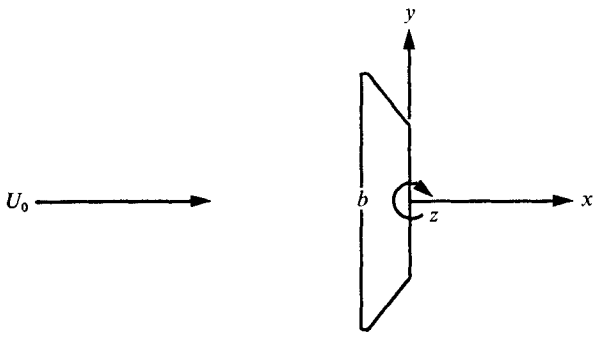

FIGURE 7. Cross-section of flat plate.

$k = 0{\cdot}5$, 1 and 2 and, for comparison, the errors for the unrectified hot wire are shown also.

With a 'rectified' hot wire, $\overline{U}_a \to 0$ as $\overline{U} \to 0$ although the ratio $\overline{U}_a/\overline{U}$ remains finite. However, in practical terms, this limiting case is not particularly important because the absolute errors from other sources, such as the straightforward confidence limit, are invariably more important once $\sigma/\overline{U}$ exceeds about 100 %, say. The results in figure 6(*a*) show rather obviously that the mean velocity errors with a rectified hot wire are much less than those from an unrectified wire at turbulent intensities greater than about 40 %. However, they are still very sensitive to k. As far as the intensity errors in figure 6(*b*) are concerned, the errors for the rectified and unrectified cases when $k = 1$ are of a very similar magnitude but opposite in sign. However, when $k = 2$, the errors with the rectified wire are actually larger than those that arise from an unrectified wire.

It appears that, even with a rectified hot-wire anemometer, the errors that arise in highly turbulent flow are quite significant. However, provided the transverse component of the turbulence is not too large, rectification does improve the accuracy of the instrument and, in view of the very widespread use of hot-wire anemometers, it might be worth developing this technique so that the range of application of the hot-wire anemometer could be extended a little further into the area of highly turbulent flows.

4. Measurements in the wake of a two-dimensional normal flat plate

Details of the experimental arrangements

The experiments were carried out in the 30 × 20 in. wind tunnel in the Mechanical Engineering Department. The cross-section of the flat plate used in the experiments is shown in figure 7 along with a definition of the co-ordinate system to be used in discussing the experimental results. The width of the flat plate was 2 in. and it spanned the 30 in. side of the wind-tunnel working section. The model was fitted with end plates.

Both the pulsed-wire and the hot-wire anemometer were operated on-line with a programmable desk calculator. In the case of the hot wire, the output from the constant-temperature anemometer unit was fed directly into an analog-to-digital

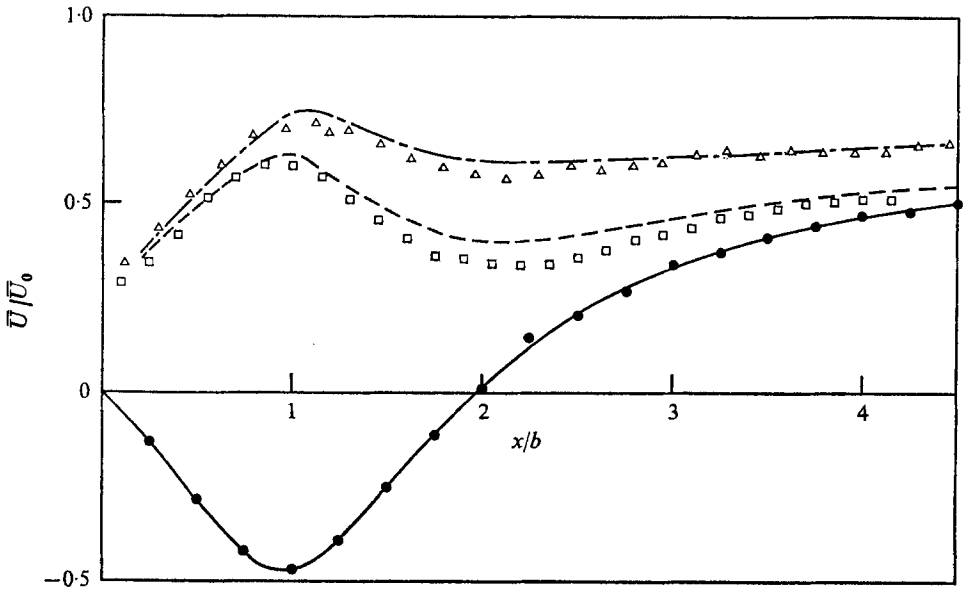

FIGURE 8. Mean velocity measurements downstream of the flat plate ($y/b = 0$). △, hot wire with axis in z direction; □, hot wire with axis in y direction; ●, pulsed wire; — · —, – – –, calculated hot-wire response.

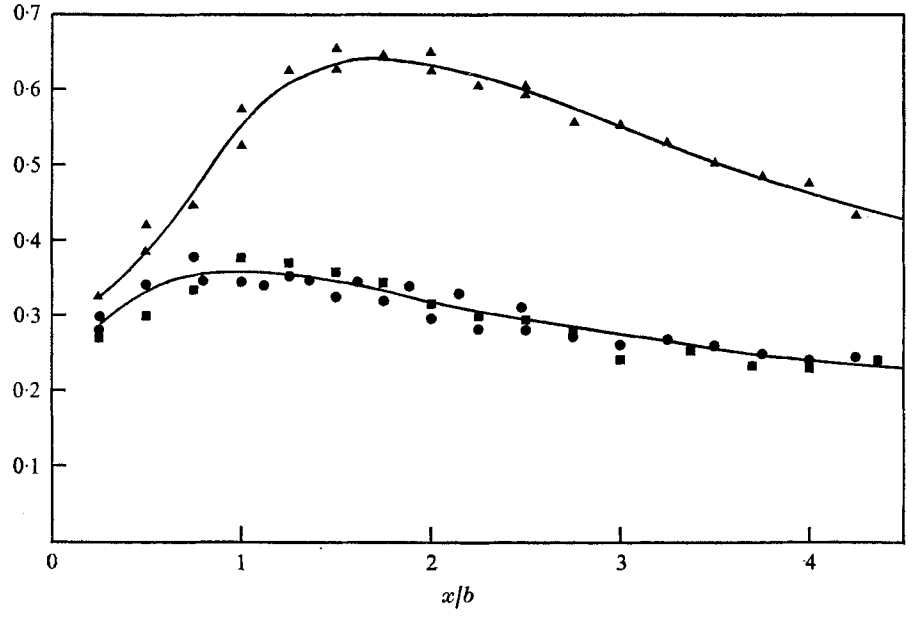

FIGURE 9. Pulsed-wire measurements of the three turbulent intensity components on wake centre-line ($y/b = 0$). ●, σ_u/U_0; ▲, σ_v/U_0; ■, σ_w/U_0.

converter and the calculator performed the linearization of each individual reading. The calculator program controlled both the number and the rate of readings and presented on-line values of mean velocity, turbulent intensity and, if required, probability density distributions. In addition to analysing the data from the experiments, the calculator also controlled the movement of the traversing gear, so that the entire experiment was automatic.

The experiments were carried out with a free-stream velocity of 7·5 m/s corrected for blockage. The sampling period for both instruments at each measuring station was about 3 min with sample sizes generally of 1000 readings. With this sample size, the 95 % confidence interval for the intensity measurements is about ± 4 % and for the mean velocity is about ± 6 % of the local turbulent intensity.

The experimental results

It should be noted that the results obtained in this section are taken from a more general investigation of the flow about a normal flat plate. However, only those results which contribute to the present discussion about the measuring devices have been included.

Figures 8 and 9 show the results of pulsed-wire measurements on the centre-line of the flow downstream of the flat plate. In these figures, $\overline{U}$ is now the measured mean velocity in the streamwise (x) direction, U_0 is the free-stream velocity and σ_u, σ_v and σ_w are the measured values of the r.m.s. intensities in the x, y and z directions respectively. The σ_v and σ_w intensities were measured simply by rotating the pulsed-wire probe such that the normal to the plane that is parallel to all three wires was aligned with the y and z directions respectively. The mean velocity variation in figure 8 shows that the reverse-flow region extends up to about two plate widths downstream and is characterized by very high reverse-flow mean velocities of about 50 % of the free-stream velocity. The interesting feature of the turbulent intensity results in figure 9 is that, whereas the u and w components of the turbulent intensity are very similar to one another, the transverse (v) component is much larger, being about twice the magnitude of the other two components for $x/b > 1{\cdot}0$. Using a potential–flow Kármán vortex street model, it is not difficult to show that such anisotropy can arise in a vortex-shedding flow (Davies 1975) and the results are therefore perhaps not as surprising as they first seem.

The high degree of anisotropy in the near wake is particularly appropriate for the purposes of the present tests because, as the hot-wire results in figures 8 and 10 show, the apparent mean velocities and turbulent intensities recorded by a hot wire with its axis normal to the mean flow direction depend on the orientation of the wire. The results shown in figures 8 and 10 were obtained with the wire aligned along the spanwise (z) direction in one case and along the transverse (y) direction in the other. They show clearly how the anisotropy of the turbulence influences the readings. It is particularly interesting in the case of the intensity measurements shown in figure 10 that not only are there differences in the magnitudes of the two sets of hot-wire results but even the forms of the variation with x/b differ from one another. This provides a strong caution against even the most qualitative interpretation of hot-wire data in highly turbulent flows.

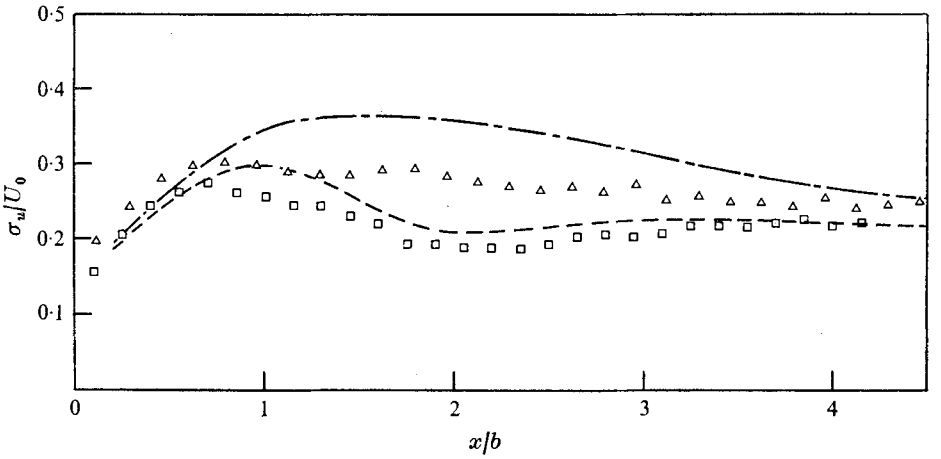

FIGURE 10. σ_u measurements with a hot-wire anemometer downstream of a flat plate. Notation as in figure 8.

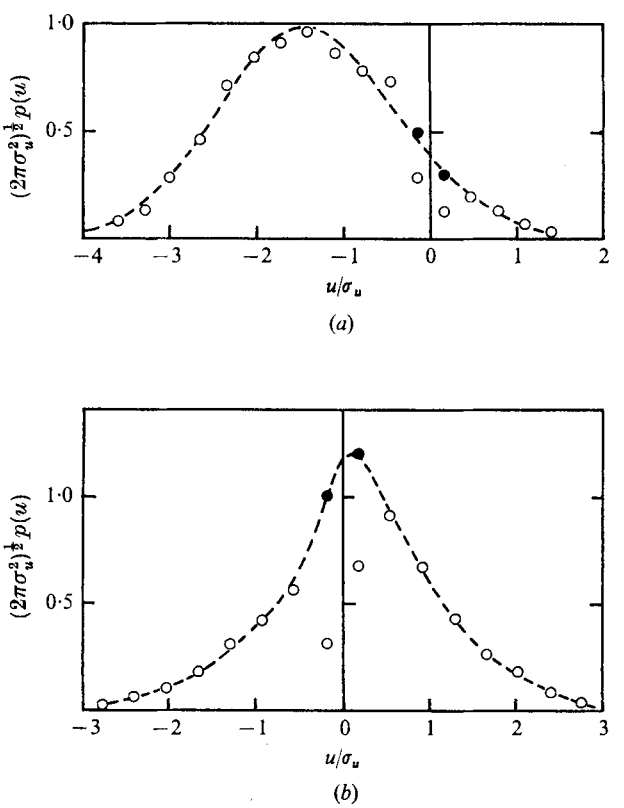

FIGURE 11. Probability density distributions on the wake centre-line. (Filled symbols include zero-velocity samples.)

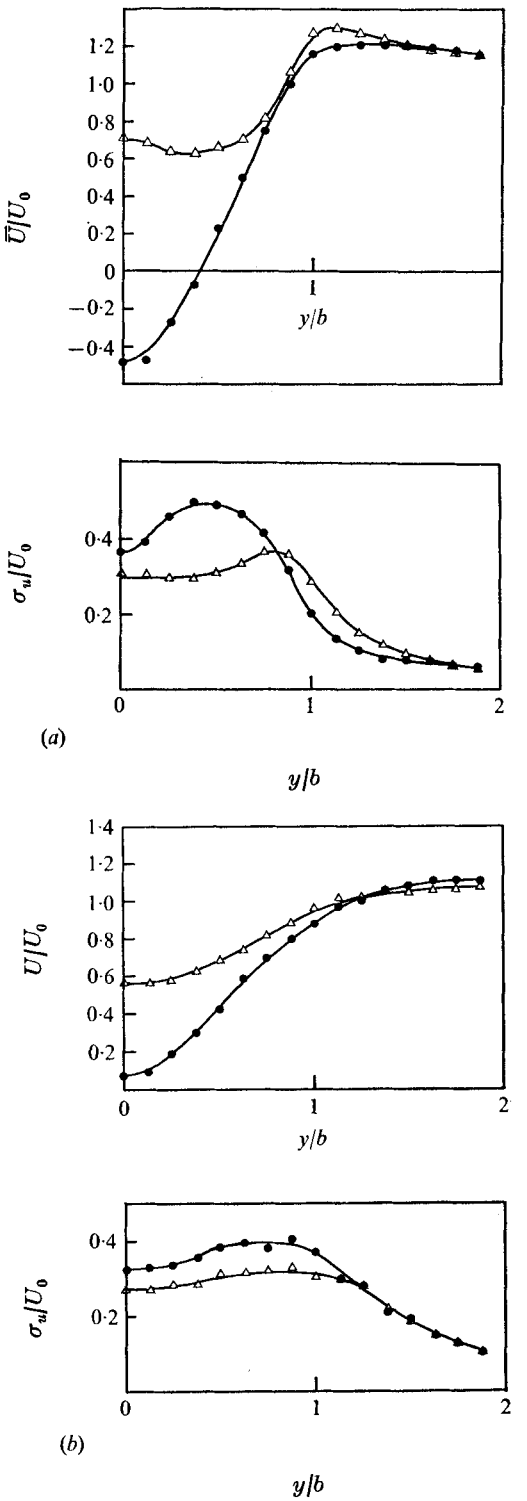

FIGURE 12. Mean velocity and turbulent intensity measurements across the wake of the plate at (*a*) $x/b = 1$ and (*b*) $x/b = 2$. ●, pulsed wire; △, hot wire.

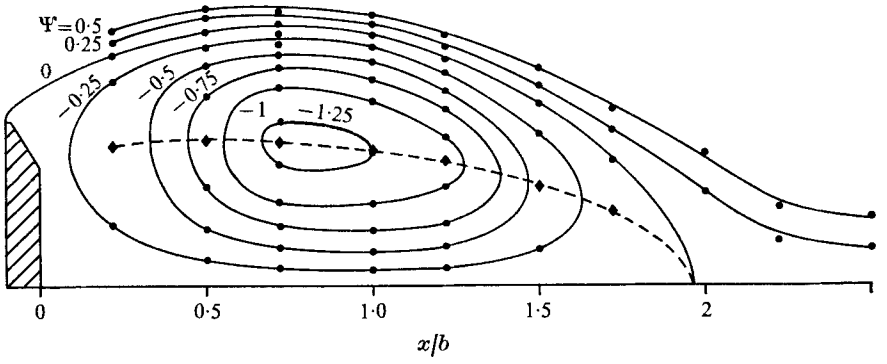

FIGURE 13. Streamline pattern in the wake of a flat plate. —, streamlines,

$$\Psi = \int_0^{y/b} (\bar{U}/U_0) d(y/b);$$

– – –, locus of zero streamwise velocity.

From the discussions in § 3, it would clearly be very difficult even to attempt to correct the hot-wire results using only the data provided by the hot-wire measurements themselves. However, in the present case, we may use the pulsed-wire measurements to calculate the hot-wire response using (11) and (12). The solid lines drawn through the pulsed-wire data in figures 8 and 9 have been used for these calculations. As far as the mean velocity calculations in figure 8 are concerned, the agreement with the experimental hot-wire data is really very good. The agreement with the hot-wire turbulent intensity measurements in figure 10 is less close but the general form of the distributions is again produced in surprising detail.

An assumption in the hot-wire analysis in § 3 was that the probability density distributions of the velocity fluctuations could be represented by uncorrelated Gaussian distributions. The probability density distributions on the wake centreline should certainly be uncorrelated with one another and in order to check the normality of the distributions, two u-component probability density distributions were obtained with the pulsed-wire anemometer on the centre-line at $x/b = 1$ and $x/b = 2$. These distributions were obtained from 10000 velocity samples divided into twenty velocity slots. The time-of-flight counter on the pulsed-wire anemometer unit was limited to a maximum time of flight of 10 ms and tracers that did not arrive within this interval were counted as zero-velocity samples. As discussed in appendix B, the finite extent of the yaw response and the departures from the cosine law both result in indentations in the measured distributions in the neighbourhood of the zero-velocity axis, and the two distributions shown in figures 11 (*a*) and (*b*) clearly demonstrate this effect. The technique that has been adopted to correct the distributions for this effect is to partition the number of missed tracers, on a trial-and-error basis, between the two points in the distributions on either side of the zero-velocity axis until plausible and apparently continuous distributions are obtained. This is obviously not a very satisfactory process and a more precise approach to this problem is being sought using the type of analysis contained in appendix B. However, for the moment, the results

in figures 11 (*a*) and (*b*) show that the centre-line probability distributions are surprisingly symmetrical and, although the distribution at $x/b = 2$ is showing departures from a Gaussian distribution, the distribution at $x/b = 1$ is apparently quite close to a normal distribution, so that the Gaussian assumption is probably not too unreasonable for the purposes of the present calculations. In addition, when one considers that probe interference effects and tangential cooling have been neglected in the analysis of § 3, it is not surprising that there are small differences between the calculated and measured hot-wire results, and in all these circumstances, the agreement provides strong evidence that the accuracy of the pulsed-wire anemometer measurements is not too different from the values suggested in § 2. Some scepticism has been expressed about the accuracy of the pulsed-wire three component intensity measurements and the marked anisotropy that these measurements appear to reveal. However, these criticisms would be difficult to sustain in view of the corroborative evidence provided by the present comparative measurements with the hot-wire anemometer.

For a final comparison, figures 12 (*a*) and (*b*) show results of measurements with a pulsed-wire and a hot-wire anemometer across the wake of the flat plate at distances downstream of $x/b = 1$ and 2 respectively. In these experiments, the axis of the hot wire was aligned with the transverse (y) direction. At the extreme edge of the flow, the pulsed-wire and hot-wire anemometers are in good agreement with one another, which again provides some welcome confirmation of the general accuracy of the experiments. The only surprising feature of these results is to be found in the differences that develop between the two instruments at $x/b = 1$ in the region from about $y/b = 1$ to $y/b = 1{\cdot}5$. Although the turbulence levels are still only about 20 % in this region, there are consistent and significant differences, particularly in the turbulent intensity results. However, the probability density distributions in this region become very skewed in a way that results from velocity 'spikes' occurring in the reverse flow direction. This will lead to errors in the hot-wire data even at these low intensities and is almost certainly responsible for the discrepancies between the two instruments.

From traverse results of the sort shown in figures 12 (*a*) and (*b*) the mean streamline pattern in the wake of the plate has been constructed as shown in figure 13. The filled circular symbols are the experimental values of the stream function obtained by integrating the velocity distributions across the wake. This procedure is sensitive to any consistent errors, for example in the probe calibration, but, in general, plausible streamlines may be drawn through the points. Also shown is the locus of zero streamwise mean velocity. This should cross the streamlines at right angles. Figure 13 demonstrates the type of measurement that can be carried out with the pulsed-wire anemometer although these particular results have only a limited value in themselves. However, the main emphasis is now being placed on conditional measurements in which velocity samples are recorded at particular phases in the vortex-shedding cycle using a hot-wire anemometer outside the wake as the synchronizing signal in a manner similar to that already used by Davies (1975).

5. Concluding remarks

This paper has been concerned with studying the behaviour of the hot-wire anemometer and the pulsed-wire anemometer in highly turbulent flow. The possibility of extending the application of the hot-wire anemometer to more highly turbulent flows by developing a scheme of simple corrections has been shown to be impractical and, moreover, even a qualitative interpretation of hot-wire data in such flows has been demonstrated to be an incautious activity.

As far as the pulsed-wire anemometer is concerned, some attempt has been made to extend the examination of its response in a highly turbulent flow and, within the limitations of the analysis, it does seem that the instrument should be capable of yielding estimates of mean velocity and turbulent intensity with an accuracy of better than 10 % in the case when the mean velocity is normal to the plane of the probe irrespective of the turbulence level. For the measurement of transverse intensities when the plane of the probe is parallel to the mean velocity direction, an accuracy of about 10 % for the turbulent intensity is still attainable provided the intensity relative to the mean velocity is greater than about 50 %. The good agreement obtained between the hot-wire results and the hot-wire response calculated using the pulsed-wire measurements also provides some useful indication of the general accuracy of the pulsed-wire anemometer measurements.

There are a number of important extensions to the range of applicability of the pulsed-wire anemometer that are currently being examined. One important area is the measurement of turbulence spectra. The recent paper by Gaster & Roberts (1975) on random sampling suggests a number of possible ways of obtaining spectra with the pulsed wire which are essentially free of aliasing errors even though the mean sampling rate is well below the frequency of turbulent motions present in the flow. Some preliminary experiments have already been carried out which demonstrate the essential feasibility of these techniques (Gaster & Bradbury 1976). It is also possible to make measurements of turbulent shear stress but, at the moment, it is not clear how the departures from the yaw response will affect the accuracy of such measurements.

Appendix A. Errors due to the finite yaw response when the mean velocity is in the plane of the probe

When the mean velocity is in the plane of the probe, the turbulent intensity measured in an isotropic Gaussian turbulence field is given by

$$\sigma_a^2 = \frac{1}{(2\pi\sigma^2)^{\frac{3}{2}}} \iiint_{\text{cones}} u^2 \exp\left(\frac{-u^2-(v-\overline{V})^2-w^2}{2\sigma^2}\right) du\,dv\,dw. \tag{A 1}$$

Only the finite extent of the yaw response is taken into account in this expression and the effect of departures from the cosine law are neglected. If polar co-ordinates are introduced such that $u = v_r \cos\theta, v = v_r \sin\theta \sin\phi, w = v_r \sin\theta \cos\phi$ and $du\,dv\,dw = v_r^2 \sin\theta\, dv_r\, d\theta\, d\phi$, it is possible to integrate (A 1) with respect to

v_r from $-\infty$ to $+\infty$. This gives finally

$$\frac{\sigma_a^2}{\sigma^2} = \frac{8\exp(-\bar{V}^2/2\sigma^2)}{\pi}\int_0^{\frac{1}{2}\pi}\int_0^{\theta}\cos^2\theta\sin\theta\exp\left(\frac{(\bar{V}\sin\theta\sin\phi)^2}{2\sigma^2}\right) \times\left\{\frac{3}{4}+3\frac{(\bar{V}\sin\theta\sin\phi)^2}{2\sigma^2}+\frac{(\bar{V}\sin\theta\sin\phi)^4}{(2\sigma^2)^2}\right\}d\theta\,d\phi, \quad \text{(A 2)}$$

where the upper limit of the integration with respect to θ is the semi-angle of the yaw response cone. This expression cannot be integrated directly for general values of $\sigma/\bar{V}$ but it has been evaluated numerically and the results are shown in figure 4.

Appendix B. The effect of the finite yaw response and departures from the cosine law on probability density distributions obtained with a pulsed-wire anemometer

We shall consider the case in which the mean velocity is in the x direction, normal to the plane of the probe. The joint probability density distribution in terms of the velocity components u and $v_r = (v^2+w^2)^{\frac{1}{2}}$ for an uncorrelated isotropic Gaussian turbulence field is

$$p(u, v_r) = \frac{v_r\exp(-v_r^2/2\sigma^2)\exp[-(u-\bar{U})^2/2\sigma^2]}{(2\pi)^{\frac{1}{2}}\sigma^3}. \quad \text{(B 1)}$$

The effective u-component velocity measured by a pulsed-wire anemometer is $u_e = u+\epsilon v_r$ and in order to determine the probability density distribution $p(u_e)$ in terms of this effective velocity, it is necessary to integrate (B 1) with respect to v_r for a constant value of u_e up to the yaw limit of the probe. The upper limit on the integration with respect to v_r is therefore $u\tan\theta$, where θ is the maximum yaw angle at which tracers can be picked up. For a constant value of u_e, this upper limit therefore becomes $(u_e\tan\theta)/(1+\epsilon\tan\theta) = V$, say, and, from (B 1), we obtain the expression

$$p(u_e) = \frac{1}{(2\pi\sigma^2)^{\frac{1}{2}}}\int_0^V \frac{v_r\exp(-v_r^2/2\sigma^2)\exp[-(u_e-\epsilon v_r-\bar{U})^2/2\sigma^2]}{\sigma^2}dv_r. \quad \text{(B 2)}$$

This may be integrated to give

$$p(u_e) = \frac{\exp[-(u_e-\bar{U})^2/2\sigma^2]}{(2\pi\sigma^2)^{\frac{1}{2}}(1+\epsilon^2)} \times\left\{\left[1-\exp\left(-\frac{1}{2\sigma^2}\left(\frac{(1+\epsilon^2)u_e^2\tan^2\theta}{(1+\epsilon\tan\theta)^2}-\frac{2\epsilon u_e(u_e-\bar{U})\tan\theta}{1+\epsilon\tan\theta}\right)\right)\right] +\frac{\epsilon(u_e-\bar{U})\pi^{\frac{1}{2}}}{[2\sigma^2(1+\epsilon^2)]^{\frac{1}{2}}}\left[\mathrm{erf}\left(\frac{(1+\epsilon^2)u_e\tan\theta/(1+\epsilon\tan\theta)-\epsilon(u_e-\bar{U})}{[2\sigma^2(1+\epsilon^2)]^{\frac{1}{2}}}\right) +\mathrm{erf}\left(\frac{\epsilon(u_e-\bar{U})}{[2\sigma^2(1+\epsilon^2)]^{\frac{1}{2}}}\right)\right]\exp\left(\frac{\epsilon^2(u_e-\bar{U})^2}{2\sigma^2(1+\epsilon^2)}\right)\Bigg\}. \quad \text{(B 3)}$$

It should be noted that when $\epsilon = 0$ equation (B 3) becomes

$$p(u_e) = \frac{\exp[-(u_e-\overline{U})^2/2\sigma^2]}{(2\pi\sigma^2)^{\frac{1}{2}}}[1-\exp(-u_e{}^2\tan^2\theta/2\sigma^2)] \tag{B 4}$$

and when $\theta = \frac{1}{2}\pi$ equation (B 3) becomes

$$p(u_e) = \frac{\exp[-(u_e-\overline{U})^2/2\sigma^2]}{(1+\epsilon^2)(2\pi\sigma^2)^{\frac{1}{2}}}\left\{\left[1-\exp\left(\frac{-u_e^2(1-\epsilon^2)+2\epsilon^2u_e\overline{U}}{2\epsilon^2\sigma^2}\right)\right]+\frac{\epsilon(u_e-\overline{U})\pi^{\frac{1}{2}}}{[2\sigma^2(1+\epsilon^2)]^{\frac{1}{2}}}\right.$$

$$\left.\times\left[\operatorname{erf}\left(\frac{u_e+\epsilon^2U}{\epsilon[2\sigma^2(1+\epsilon^2)]^{\frac{1}{2}}}\right)+\operatorname{erf}\left(\frac{\epsilon(u_e-\overline{U})}{[2\sigma^2(1+\epsilon^2)]^{\frac{1}{2}}}\right)\right]\exp\left(\frac{\epsilon^2(u_e-\overline{U})^2}{2\sigma^2(1+\epsilon^2)}\right)\right\}. \tag{B 5}$$

It should also be noted that the probability of missing a tracer is independent of the value of ϵ, so that

$$\int_{-\infty}^{\infty}p(u)\,du = \int_{-\infty}^{\infty}p(u_e)\,du_e = 1-\cos\theta\exp\left(\frac{-\sin^2\theta}{2(\sigma^2/\overline{U}^2)}\right) \tag{B 6}$$

for a given value of θ.

In order to illustrate the effect of the finite yaw response and departures from the cosine law on probability density distributions, two cases will be considered, namely when $\overline{U}/\sigma = 0$ and when $\overline{U}/\sigma = 1$. Figures 14 (*a*) and (*b*) show calculated probability density distributions for these two cases. We shall consider first the effect of the finite yaw response only (i.e. $\epsilon = 0$) using (B 4). It should be noted from (B 4) that $p(u_e) = 0$ when $u_e = 0$ and that the effect of the finite yaw response is to cause the probability density distributions to dip to zero when $u_e = 0$. The width of this indentation in the distributions is of the order of $\pm u_e/\sigma = 2/\tan\Theta$ taking ϵ^{-2} as a measure of 'smallness'. Figures 14 (*a*) and (*b*) show the results of calculations using (B 4) for the case when $\theta = 70°$. We can now examine the effect of departures from the cosine law, and figures 14 (*a*) and (*b*) also show results for the case when $\theta = 70°$ and $\epsilon = 0{\cdot}1$ calculated from (B 3). The effect of the departures from the cosine law is to broaden further the indentation in the distributions and, in fact, for practical values of ϵ and θ, the width of the indentation is now of the order of $\pm u_e/\sigma = 2(1+\epsilon\tan\theta)/\tan\theta$. It should be noted that the area under the probability density distributions is unaffected by the value of ϵ in accordance with (B 6). Figures 14 (*a*) and (*b*) also show results for the case when $\theta = 90°$ and $\epsilon = 0{\cdot}1$ calculated from (B 5). It will be seen that the departures from the cosine law alone cause a dip in the probability density distributions. $p(u_e)$ is again zero when $u_e = 0$. It should also be noted that the distributions when $\epsilon \neq 0$ merge when $|u_e/\sigma| > 2(1+\epsilon\tan\theta)/\tan\theta$ since (B 5) behaves like

$$p(u_e) = \frac{\exp[-(u-\overline{U})^2/(2\sigma^2)]}{(2\pi\sigma^2)^{\frac{1}{2}}}\left(1+\frac{\epsilon|u_e-\overline{U}|\pi^{\frac{1}{2}}}{(2\sigma^2)^{\frac{1}{2}}}\right),$$

where terms containing ϵ^2 have also been neglected since $\epsilon^2 \ll 1$. This limiting case is independent of the value of θ.

The effect of imperfections in the yaw response can be seen in the practical distributions shown in figure 11. With real probes, the two sensor wires are not

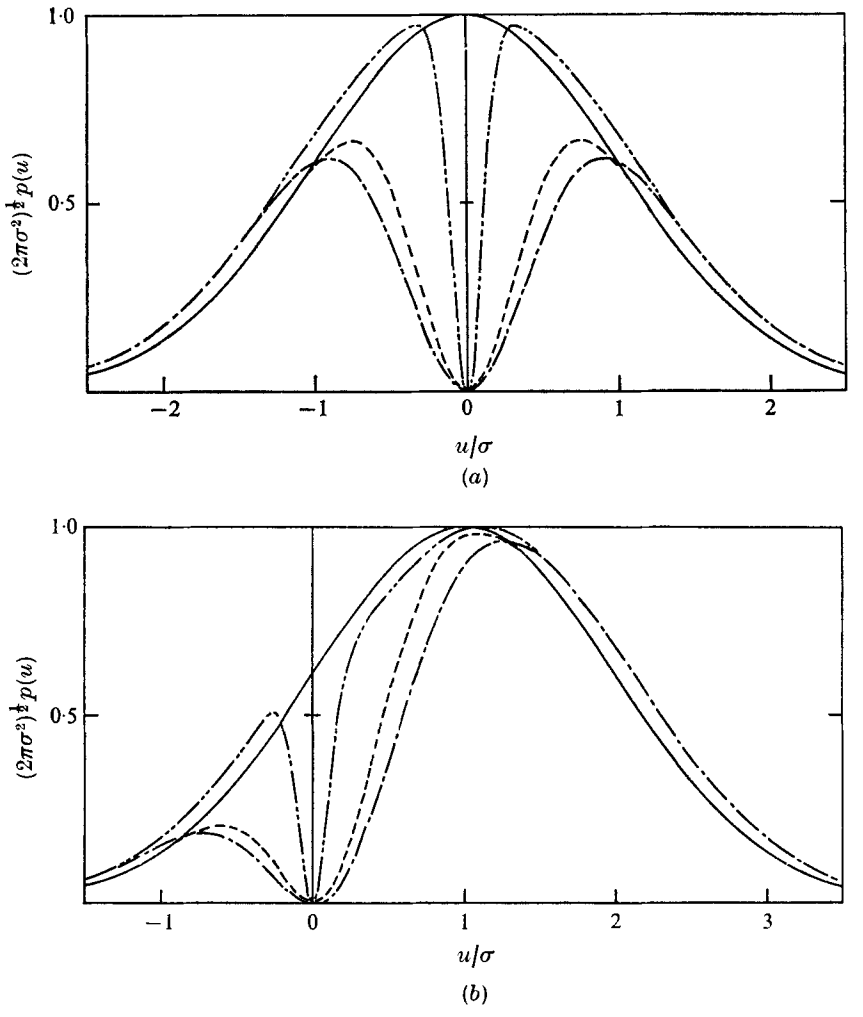

FIGURE 14. The effect of finite yaw response and departures from the cosine law on probability density distributions. (*a*) $\bar{U}/\sigma = 0$. (*b*) $\bar{U}/\sigma = 1$. —, Gaussian distribution; – – –, $\theta = 70°$, $\epsilon = 0$; — · —, $\theta = 70°$, $\epsilon = 0{\cdot}1$; — · · —, $\theta = 90°$, $\epsilon = 0{\cdot}1$.

symmetrical, so that the width of the indentations on either side of the $u_e = 0$ axis are not necessarily the same. However, the probe used to obtain the results shown in figure 11 had a yaw response that extended up to approximately 70° and, as reference to figures 14(*a*) and (*b*) will show, it is not too difficult in such cases to distribute the zero-velocity samples over the region of the indentations to produce plausible although slightly incorrect probability density distributions. This is obviously a rather crude procedure and difficulties can arise with probes with a very wide yaw response extending up to 80° or more because the width of indentations is more dependent on the value of ϵ than it is on the value of θ. In these cases the number of zero-velocity samples is insufficient to 'fill in' the indentations in the probability density distributions. However, it may be possible to use the results of the present analysis to devise a more precise means of cor-

recting the probability density distributions and this possibility will be explored in future work.

Finally, it should be noted that (B 3) may be used in the normal way to compute apparent mean velocities and turbulent intensities recorded by the pulsed-wire anemometer for arbitrary values of ϵ and θ. However, the results of such calculations do not affect the conclusions contained in the main text and, for simplicity, they have not been included.

REFERENCES

BRADBURY, L. J. S & CASTRO, I. P. 1971 A pulsed-wire technique for velocity measurements in highly turbulent flows. *J. Fluid Mech.* **49**, 657.

BRADBURY, L. J. S. & MOSS, W. D. 1975 Pulsed wire anemometer measurements in the flow past a normal flat plate in uniform flow and in sheared flow. *Proc. 4th Int. Conf. Wind Effects on Buildings & Structures, London.*

COOK, N. J. & REDFEARN, D. 1976 The calibration and use of a hot wire probe for highly turbulent and reversing flows. *J. Ind. Aerodyn.* **1**, 221.

DAVIES, M. E. 1975 Wakes of oscillating bluff bodies. Ph.D. thesis, Aeronautics Department, Imperial College.

DOWNING, P. M. 1972 Reverse flow sensing hot wire anemometer. *J. Sci. Instrum.* **5**, 819.

GASTER, M. 1971 Vortex shedding from slender cones. *Proc. UITAM Symp. Recent Res. on Unsteady Boundary Layers*, vol. 2, p. 499.

GASTER, M. & BRADBURY, L. J. S. 1976 The measurement of the spectra of highly turbulent flows by a randomly triggered pulsed-wire anemometer. *J. Fluid Mech.* **77**, 499.

GASTER, M. & ROBERTS, J. B. 1975 Spectral analysis of randomly sampled signals. *J. Inst. Math. Appl.* **15**, 195.

GUENKEL, A. A., PATEL, R. P. & WEBER, M. E. 1971 A shrouded hot-wire probe for highly turbulent flows and rapidly reversing flows. *Ind. Engng Chem. Fund.* **10**, 627.

TANI, I., IUCHI, M. & KOMODA, H. 1961 Experimental investigations of flow separation over a step. *Aero. Res. Inst., Univ. Tokyo Rep.* no. 364.

TUTU, N. K. & CHEVRAY, R. 1975 Cross-wire anemometry in high intensity turbulence. *J. Fluid Mech.* **71**, 785.